This article has been accepted for publication in a future issue of this journal, but has not been fully edited. Content may change prior to final publication. Citation information: DOI 10.1109/TAP.2019.2955219, IEEE Transactions on Antennas and Propagation

Dynamically Realizing Arbitrary Multi-Bit Programmable Phases Using a 2-Bit Time-Domain Coding Metasurface

Lei Zhang, Zheng Xing Wang, Rui Wen Shao, Jia Lin Shen, Xiao Qing Chen, Xiang Wan, *Member, IEEE*, Qiang Cheng, *Member, IEEE*, and Tie Jun Cui, *Fellow, IEEE*

***Abstract*—Recently, digital coding metasurfaces have attracted significant attention due to their capability to dynamically control electromagnetic waves in programmable ways. When the digital bit of a metasurface is higher, its controlling capability will be stronger. However, it is extremely difficult to realize 3-bit and higher digital coding metasurfaces since an *n*-bit digital element will require many active devices (e.g. PIN diodes) to achieve 2^n digital states. Here, we propose to realize arbitrary multi-bit programmable phases using 2-bit time-domain digital coding metasurface at the central frequency or harmonic frequencies. We introduce the method of vector synthesis to design the phase coverages, from which 4-bit and arbitrarily higher-bit coding phases are synthesized by a physical coding metasurface with only 2-bit phases, simply by manipulating the time-coding sequences. A prototype controlled by a field-programmable gate array is used to validate this methodology. Experimental results are in good agreement with the theoretical analysis, which demonstrate good performance of the proposed method in dynamically realizing arbitrary multi-bit programmable phases. This time-varying coding strategy provides a new way to design higher-bit programmable metasurface and simplify the structural design and control system, which will find many potential applications such as high-resolution imaging and high-capacity wireless communications.**

***Index Terms*—Digital coding metasurface, multi-bit phases, programmable, quantization error, time-varying.**

I. Introduction

Metasurfaces are artificially engineered 2D structures that have attracted great attention in both science and engineering communities owing to their attractive features, including ultrathin thickness, low loss, easy fabrication and good integrability [1], [2]. Metasurfaces have been widely used to manipulate electromagnetic (EM) waves in unconventional ways, leading to many exotic physical phenomena and interesting devices capable of manipulating microwaves [3], terahertz waves [4], [5], visible light [6], [7] and acoustic waves [8]. As the digital version of metasurface, digital coding and programmable metasurfaces have rapidly developed since they were proposed by Cui *et al.* in 2014 [9]. Coding metasurface consists of a limited numbers of elements and can control EM waves in a discretized and digital manner, which has the advantage to simplify design and optimization procedures and have many functionalities in programmable ways [10]-[19]. For example, for an *n*-bit digital coding metasurface, each element consists of 2^n digital states with the phase interval of $2\pi/2^n$. The digital representation of coding metasurfaces is essentially suitable for integrating active devices, thereby leading to programmable metasurfaces [9], [20]-[25].

So far, 1-bit and 2-bit programmable metasurfaces have been successfully realized by using active devices (e.g. PIN diodes) and field programmable gate array (FPGA) [20]-[25]. It is well known that higher-bit programmable metasurfaces have lower quantization phase error and can control EM waves more precisely, and hence have stronger capability to manipulate EM waves [26-28]. However, it is very challenging to achieve multi-bit programmable phases via the PIN-diode-based metasurfaces. For example, a 3-bit digital element requires three PIN diodes to achieve the eight digital states 000, 001, 010, 011, 100, 101, 110, and 111; and an *n*-bit digital element requires *n* PIN diodes to achieve the 2^n digital states. Thus the structural design, biasing circuit, and control system will be very complicated for the higher-bit digital coding metasurfaces. Another way to realize the higher-bit programmable metasurface is to use varactors [29]-[33], but it is typically accompanied by higher losses. Moreover, the varactors need higher biasing voltages and extra carefully-designed driving circuits, in which the switching speed is very limited. More recently, some other techniques have been subsequently suggested to design programmable metasurfaces, such as MEMS [34], graphene [35], liquid crystal [36], and other mechanisms [37], [38], but they are further away from practical usages. More importantly, all these studies have limited phase coverages.

On the other hand, time-varying metasurfaces have recently attracted an increasing interest, owing to their capacity to manipulate the time dimension of EM waves by modulating the metasurface properties in the time domain [32], [33], [39]-[45].

This work was supported in part by the National Key Research and Development Program of China (Grant Nos. 2017YFA0700201, 2017YFA0700202, and 2017YFA0700203), in part by the National Natural Science Foundation of China (Grant Nos. 61631007, 61571117, 61501112, 61501117, 61522106, 61731010, 61735010, 61722106, 61701107, and 61701108), in part by the 111 Project (Grant No. 111-2-05), in part by the Fund for International Cooperation and Exchange of the National Natural Science Foundation of China (Grant Nos. 61761136007), in part by the Postgraduate Research & Practice Innovation Program of Jiangsu Province (KYCX18_0097), and in part by the Scientific Research Foundation of Graduate School of Southeast University (YBPY1858). (*Corresponding author: Tie Jun Cui.)*

The authors are with the State Key Laboratory of Millimeter Waves, Southeast University, Nanjing 210096, China (e-mail: zhanglei.xdu@seu.edu.cn ; tjcui@seu.edu.cn).

This article has been accepted for publication in a future issue of this journal, but has not been fully edited. Content may change prior to final publication. Citation information: DOI 10.1109/TAP.2019.2955219, IEEE Transactions on Antennas and Propagation

Time-varying approach has produced new physical phenomena and further extended the application range of the metasurface. Combined with the space modulation, space-time-modulated metamaterials have also been demonstrated that their physical properties can be controlled in both space and time domains [22], [23], [46]-[58].

The time-varying and space-time-modulated metamaterials and metasurfaces have been widely investigated in recent years, which bring many interesting applications, such as breaking time-reversal symmetry and Lorentz reciprocity [39]-[41], [46], [47], [50], Doppler cloaks [42], [51], harmonics generation [41], [52], optical isolators [39], [53], nonreciprocal antennas [54]-[56], and full-duplex systems [57], [58]. It is worth noting that most of the above time-varying and space-time-modulated structures are theoretical and numerical investigations, while only few practical realizations are demonstrated for guided waves, and experimental realization for space waves remains limited. Conversely, some realistic metasurfaces with time-varying physical parameters (e.g., reflection or transmission coefficient and surface impedance) have been experimentally demonstrated [22], [23], [32], [33], [43]-[45]. For example, the space-time-modulated coding metasurface has been proposed to enable simultaneous manipulations of EM waves in both space and frequency domains, such as harmonic beam steering [22], scattering-signature control [22], and the programmable nonreciprocal effect [23]. Besides, some varactor-based time-varying metasurfaces have been developed for new architecture of wireless communication [32], harmonics control [33], frequency conversion [43], [44], and nonreciprocal wavefront engineering [45]. The time-varying approach has brought a new degree of freedom in controlling the EM waves, which motivates our study here to explore the realization of multi-bit programmable phases.

In this paper, we utilize the previously proposed 2-bit programmable metasurface combined with the time-domain coding approach, to attain arbitrary multi-bit and even quasi-continuous programmable phases by simply designing suitable 2-bit time-coding sequences. First, we present a theoretical analysis of the time-domain digital coding metasurface and introduce the method of vector synthesis to further explain the phase coverage. Subsequently, we present several examples of beam steering using 4-bit digital coding metasurfaces based on the 2-bit time-domain programmable metasurface at both central frequency and harmonic frequencies to demonstrate the effectiveness of the proposed method. Finally, we fabricate and experimentally test a prototype. The proposed methodology may find a wide range of applications including antenna arrays, imaging, radar systems, and wireless communications.

The paper is organized as follows: Section II presents the theory of the proposed multi-bit time-varying coding strategy. Section III presents the design and simulations of the 2-bit time-domain coding metasurface and its elements. In Section IV, the experimental results of proposed method are discussed, followed by the detailed analysis of its performance. Finally, conclusions are summarized in Section V.

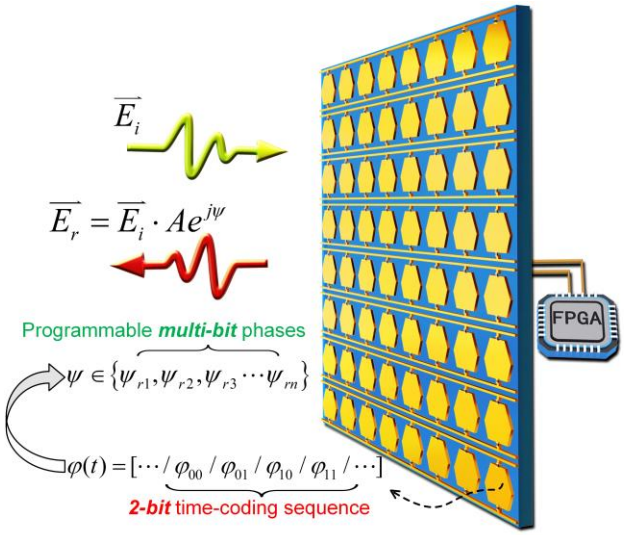

Fig. 1. Dynamic multi-bit programmable metasurface controlled by FPGA.

II. Theory and Methodology

We consider a reflection-type digital coding programmable metasurface composed of a 2D array of PIN-diode-based 2-bit digital elements, whose reflection phases are periodically switched according to the 2-bit time-coding sequence [22], as shown in Fig. 1. By applying different control voltages to the PIN diodes, the reflection phases of each element can be dynamically controlled with discrete 2-bit states (i.e., 00, 01, 10, and 11) in the physical layer. The 2-bit coding metasurface is normally illuminated by an incident monochromatic plane wave with the time-harmonic form $E_i(t)=E_0 \cdot e^{j\omega_c t}$, and the reflected wave can be expressed as

$$E_r(t) = E_i(t) \cdot \Gamma(t) \tag{1}$$

where $\Gamma(t) = \alpha(t)e^{j\varphi(t)}$ is the time-varying complex reflection coefficient, with $\alpha(t)$ and $\varphi(t)$ denoting the amplitude and phase in the time domain, respectively; and $\Gamma(t)$ is periodic in time and can be defined as $\Gamma(t)=\sum_{n=1}^{L}\Gamma^n U^n(t)$, with $U^n(t)$ denoting a periodic pulse function under the modulation period T_0. Therefore, the time-domain coding metasurface can be characterized by time-coding sequence with length L, and Γ^n is the reflection coefficient during the *n*th time interval [22].

According to the Fourier transform theory, the reflected wave in the frequency domain can be written as

$$E_r(\omega) = \frac{1}{2\pi} E_i(\omega) * \Gamma(\omega) \tag{2}$$

where $E_i(\omega) = E_0 \cdot 2\pi\delta(\omega - \omega_c)$ represents the incident wave in the frequency domain, and $\Gamma(\omega)$ is the Fourier transform of $\Gamma(t)$. We decompose the periodic function $\Gamma(t)$ into a Fourier series $\Gamma(t) = \sum_{m=-\infty}^{+\infty} a_m e^{jm\omega_0 t}$, whence $\Gamma(\omega) = 2\pi \sum_{m=-\infty}^{+\infty} a_m \delta(\omega - m\omega_0)$,

This article has been accepted for publication in a future issue of this journal, but has not been fully edited. Content may change prior to final publication. Citation information: DOI 10.1109/TAP.2019.2955219, IEEE Transactions on Antennas and Propagation

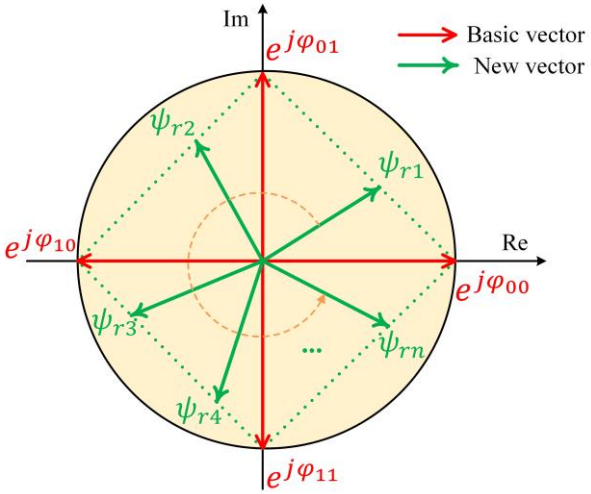

Fig. 2. The vector synthesis method in the complex plane to realize the multi-bit programmable phases.

with $\omega_0 = 2\pi/T_0$ denoting the angular modulation frequency. The Fourier coefficient a_m is given by [22]

$$a_m = \sum_{n=1}^{L} \frac{\Gamma^n}{L} \mathrm{sinc}\left(\pi m/L\right) \cdot e^{-j\pi m(2n-1)/L} = A^m e^{j\psi^m} \qquad (3)$$

which represents the complex reflection coefficient of the metasurface in frequency domain at the mth harmonic frequency $\omega_c + m\omega_0$, with the equivalent amplitude A^m and equivalent phase ψ^m. Thus, equation (2) can be further represented as

$$E_r(\omega) = E_0 \cdot \Gamma(\omega - \omega_c) = 2\pi E_0 \cdot \sum_{m=-\infty}^{+\infty} a_m \delta(\omega - \omega_c - m\omega_0) \qquad (4)$$

The spectrum of the reflected wave $E_r(\omega)$ is a superposition of fields at all harmonic frequencies $\omega_c + m\omega_0$ (m=0, ±1, ±2 …). To reach arbitrary-bit phase distributions, we can obtain the desired frequency component while suppressing other unwanted frequency components by suitably designing the time-coding sequence.

In the theoretical modeling, we consider a physical 2-bit programmable metasurface that are designed with four standard 2-bit phases "φ_{00}", "φ_{01}", "φ_{10}", and "φ_{11}", corresponding to 0°, 90°, 180°, and 270° phase responses, respectively. These 2-bit programmable phases can be switched in time under the control of FPGA. We assume that the reflection amplitudes of the 2-bit programmable metasurface are uniform and equal to 1, then the complex reflection coefficients of the time-domain metasurface at the central frequency ω_c and the first harmonic frequency $\omega_c + \omega_0$ can be derived from equation (3),

$$\begin{aligned} a_0 &= \sum_{n=1}^{L} \frac{\Gamma^n}{L} = A^0 e^{j\psi^0}, \ \Gamma^n \in \left\{ e^{j\varphi_{00}}, \ e^{j\varphi_{01}}, \ e^{j\varphi_{10}}, \ e^{j\varphi_{11}} \right\} \\ a_1 &= \sum_{n=1}^{L} \frac{\Gamma^n}{L} \mathrm{sinc}\left(\pi/L\right) \cdot e^{-j\pi(2n-1)/L} = A^1 e^{j\psi^1} \end{aligned} \qquad (5)$$

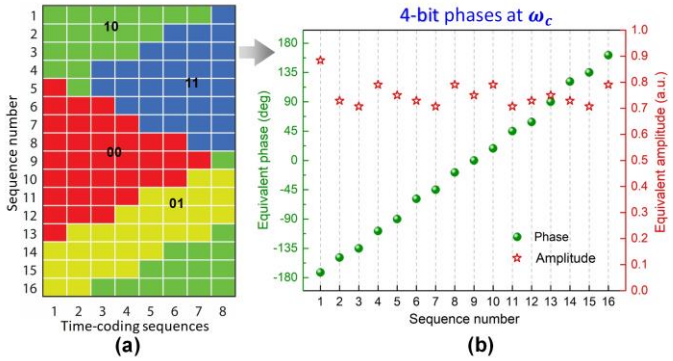

Fig. 3. (a) The optimized sixteen sets of time-coding sequences and (b) their corresponding equivalent 4-bit phases at the central frequency ω_c.

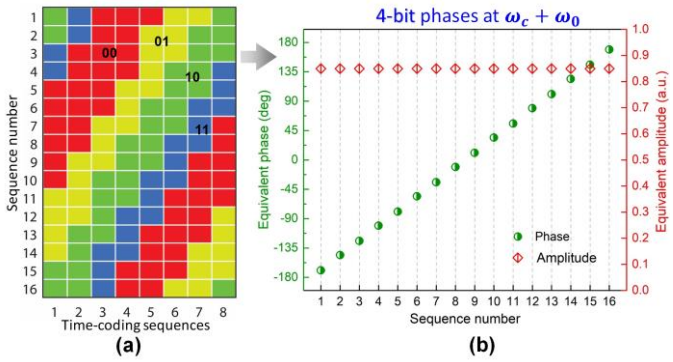

Fig. 4 (a) The optimized sixteen sets of time-coding sequences and (b) their corresponding equivalent 4-bit phases at the first harmonic frequency $\omega_c + \omega_0$.

We first study the phase coverage ψ^0 at the central frequency by introducing the method of vector synthesis. For example, if the time-coding sequence is "00-01-01-01" with length L=4, then the complex reflection coefficient a_0 in (5) is written as

$$a_0 = \frac{e^{j\varphi_{00}} + e^{j\varphi_{01}} + e^{j\varphi_{01}} + e^{j\varphi_{01}}}{4} = \frac{1}{4} e^{j\varphi_{00}} + \frac{3}{4} e^{j\varphi_{01}} \approx 0.79 e^{j71.57^\circ} \qquad (6)$$

It can be found that an equivalent phase 71.57° is successfully realized with the equivalent amplitude 0.79 at the central frequency. This means that when the 2-bit programmable metasurface is periodically switched in time according to the 2-bit phases "0°-90°-90°-90°", a differently equivalent phase 71.57° is obtained.

Moreover, we use the vector operation in the complex plane to further explore the phase coverage. Four basic vectors of the original 2-bit reflection coefficients $e^{j\varphi_{00}}$, $e^{j\varphi_{01}}$, $e^{j\varphi_{10}}$, and $e^{j\varphi_{11}}$ are depicted in Fig. 2. In the above example of time-coding sequence "00-01-01-01", the complex reflection coefficient a_0 is synthesized by adding two vectors of $e^{j\varphi_{00}}/4$ and $3e^{j\varphi_{01}}/4$, where the new vector $0.79e^{j71.57^\circ}$ with phase 71.57° is generated. If the time-coding sequence is chosen as "10-10-10-10-10-11-11-11" with length L=8, another

This article has been accepted for publication in a future issue of this journal, but has not been fully edited. Content may change prior to final publication. Citation information: DOI 10.1109/TAP.2019.2955219, IEEE Transactions on Antennas and Propagation

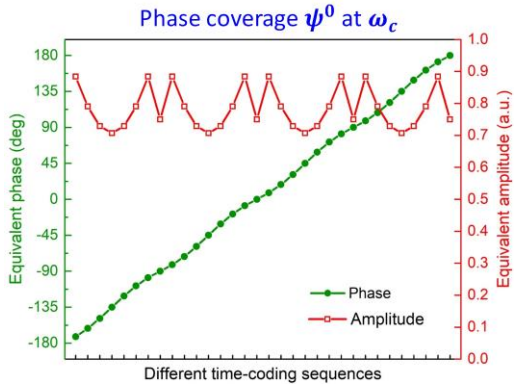

Fig. 5. The equivalent phase coverage at ω_c with equivalent amplitude greater than 0.7.

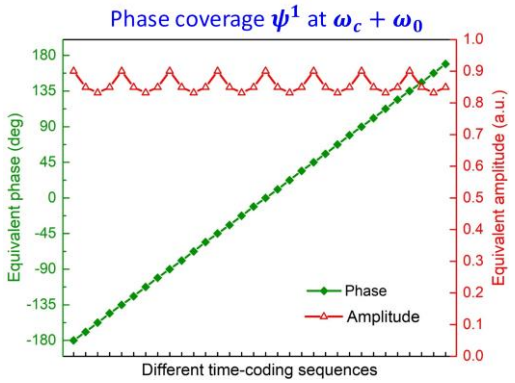

Fig. 6. The equivalent phase coverage at $\omega_c + \omega_0$ with equivalent amplitude greater than 0.83.

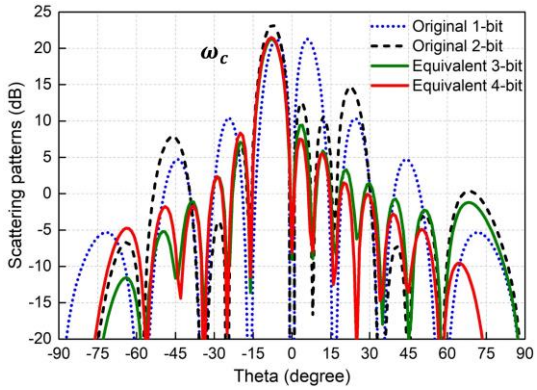

Fig. 7. Comparison of 1D scattering patterns pertaining to the original 1-bit, 2-bit and equivalent 3-bit, 4-bit phases (in Fig. 3) for beam steering at the central frequency ω_c.

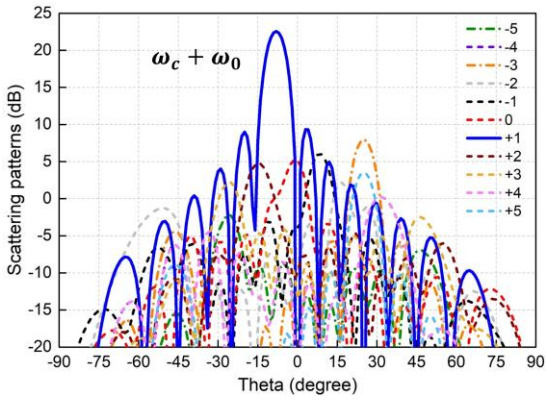

Fig. 8. 1D scattering patterns of equivalent 4-bit phases in Fig. 4 for beam steering at the first harmonic frequency $\omega_c + \omega_0$.

complex reflection coefficient is synthesized by adding two vectors of $5e^{j\varphi_{10}}/8$ and $3e^{j\varphi_{11}}/8$, where the new vector $0.73e^{j-149^\circ}$ with phase -149 ° is generated. Therefore, new vectors ($A_{rn}e^{j\psi_{rn}}$) can always be synthesized by properly combining the four basic vectors. That is to say, as long as we suitably design the 2-bit time-coding sequence, the new equivalent phases can be synthesized into arbitrary values with 360 °phase coverage, as discussed in the next section.

III. Designs and Simulations

As an example, we consider the 2-bit time-coding sequences with length L=8, represented by the color block diagram. Sixteen sets of time-coding sequences are illustrated in Fig. 3(a), which are used to attain the 4-bit digital phases (ideal 16 states: -180 °, -157.5 °, -135 °, -112.5 °, -90 °, -67.5 °, -45 °, -22.5 °, 0 °, 22.5 °, 45 °, 67.5 °, 90 °, 112.5 °, 135 °, and 157.5 °) at the central frequency ω_c. As shown in Fig. 3(b), the equivalent 4-bit phases are successfully synthesized with the amplitudes greater than 0.7 only by using the physical 2-bit phases, which are very close to the ideal digital states. Similar case can be achieved at the harmonic frequencies. Fig. 4(a) displays another sixteen sets of time-coding sequences, which are used to generate the equivalent 4-bit phases at the first harmonic frequency $\omega_c + \omega_0$, in which all amplitudes are above 0.83 and the phases are close to the ideal digital states, as shown in Fig. 4(b). In this manner, by exploring more different time-coding sequences, the phase coverage at the central frequency and the first harmonic frequency can reach 360 °with high amplitudes and more digital-bit phases, as illustrated in Fig. 5 and Fig. 6. Hence, the proposed time-varying approach provides a new way of realizing programmable quasi-continuous phase modulations. It should be mentioned that the criterion for selecting those time-coding sequences is to make the equivalent phases at the target frequency to exhibit the required multi-bit responses with high amplitudes. An in-house code based on equation (3) is generated to search for the eligible time-coding sequences.

As far as we know, higher-bit digital phases have lower quantization error than lower-bit digital phases [26]-[28]. As an illustrative example, we use the time-coding sequences in Fig. 3(a) and Fig. 4(a) to show the advantages of higher-bit digital phases in beam steering. Specifically, we consider a programmable coding metasurface consisting of 16×16 elements with the period of $0.44\lambda_c$, in which each column has the same digital code. First, we address the beam steering in one plane at the central frequency ω_c. By sequentially applying the sixteen sets of time-coding sequences in Fig. 3(a) to the 16-column elements, the metasurface has the 4-bit phase

This article has been accepted for publication in a future issue of this journal, but has not been fully edited. Content may change prior to final publication. Citation information: DOI 10.1109/TAP.2019.2955219, IEEE Transactions on Antennas and Propagation

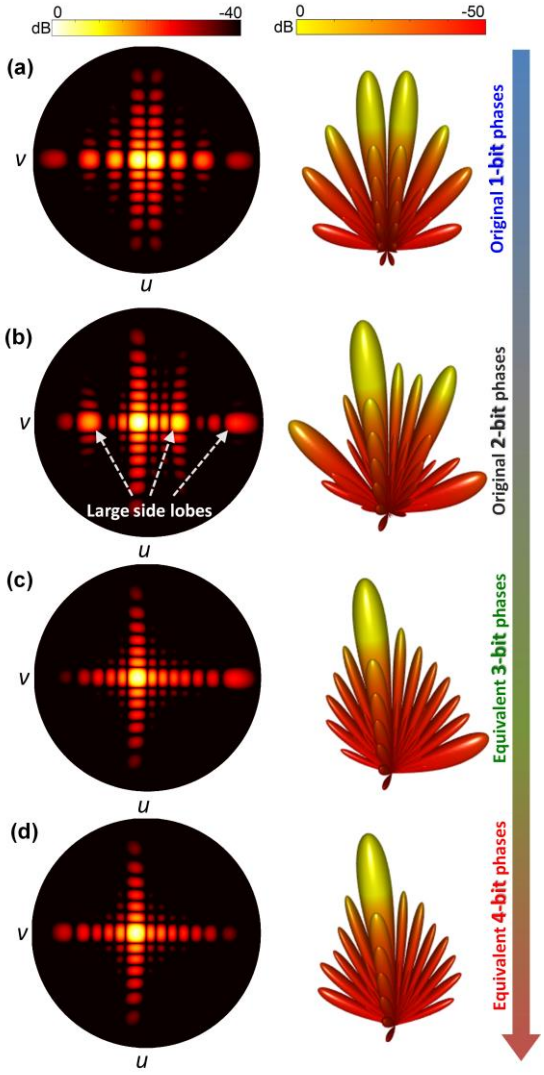

Fig. 9. The corresponding 2D and 3D scattering patterns for the beam steering in Fig. 7, pertaining to (a) original 1-bit, (b) original 2-bit, (c) equivalent 3-bit and (d) equivalent 4-bit phases at ω_c, respectively.

distribution at the central frequency. This accurately gradient phase distribution (with 16 digital states) will steer the normally incident wave to an angle of -8.1 °, as displayed in Fig. 7 (the red line) and Fig. 9(d). It can be seen that the main beam points to the angle of $\theta=-8.1^{\circ}$. Moreover, we compare the far-field scattering patterns of the equivalent 4-bit phases (see Fig. 3) with the original 1-bit phases ("0°-0 °-0 °-0 °-0 °-0 °-0 °-180 °-180 °-180 °-180 °-180 °-180 °-180 °-180°"), original 2-bit phases ("0°-0 °-0 °-0 °-90 °-90 °-90 °-90 °-180 °-180 °-180 °-180 °-270 °-270 °-270 °-270°"), and equivalent 3-bit phases, which could also realize the steering angle of -8.1 ° but will accompany by several large side lobes, as shown in Fig. 7. Figs. 9(a)-(c) show the corresponding 2D and 3D scattering patterns for the beam steering in Fig. 7. It can be seen that the original 1-bit and 2-bit phase quantization produces significant quantization lobes, which are avoided in the case of equivalent 4-bit phases.

Another example of the equivalent 4-bit phases for beam steering at the first harmonic frequency $\omega_c+\omega_0$ is illustrated in Fig. 8. We can see that the main beam at the first harmonic

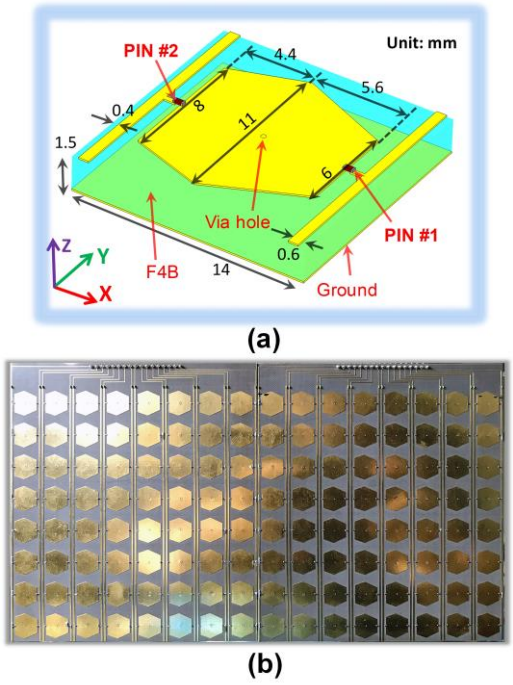

Fig. 10. (a) Geometry of the 2-bit programmable element loaded with two PIN diodes. (b) Photograph of the fabricated 2-bit programmable metasurface prototype.

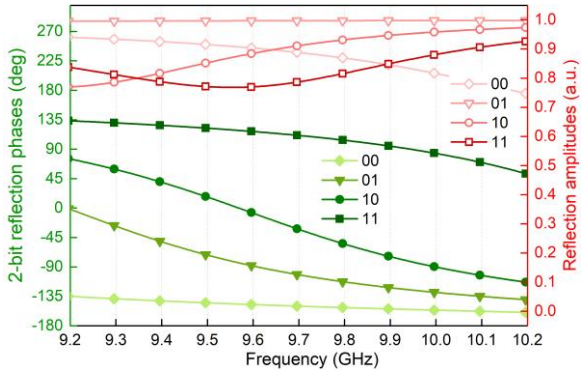

Fig. 11. Simulated reflection phases and amplitudes of the 2-bit programmable element excited by a normally incident plane wave (with *x*-polarized electric field).

frequency points to the angle of $\theta=-8.1^{\circ}$, and the other unwanted frequency components are well suppressed. Generally, the equivalent 4-bit or higher-bit programmable metasurface provides more degrees of freedom in beam steering than the 1-bit and 2-bit physical metasurface, and can control the EM waves more precisely. Actually, in the traditional field of phased-array antennas, digital phase shifters have been widely employed to control radiation patterns [59]. To reduce quantization side lobes and beam-pointing errors, higher-bit phase shifters are also needed but bring very high cost and system complexity. Thus the proposed time-varying approach provides a new method to design metasurface-based phased arrays with high-bit programmable phases, which could reduce the quantization error without using the traditional digital phase shifters.

This article has been accepted for publication in a future issue of this journal, but has not been fully edited. Content may change prior to final publication. Citation information: DOI 10.1109/TAP.2019.2955219, IEEE Transactions on Antennas and Propagation

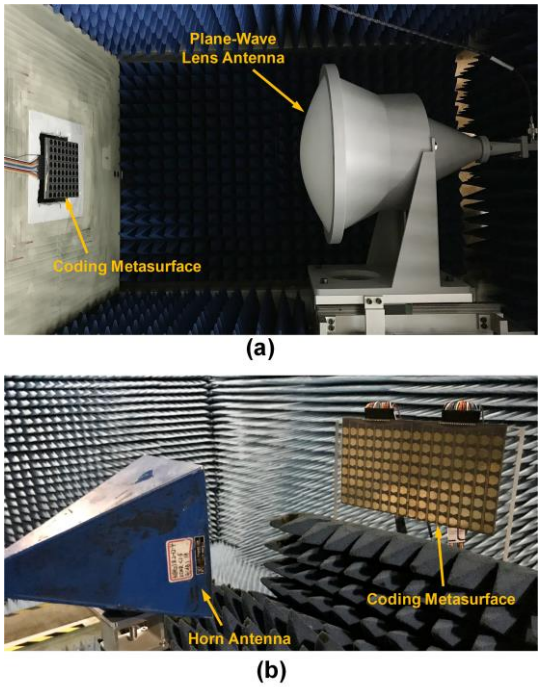

Fig. 12. Photographs of experimental setups for measuring (a) the reflection phases, and (b) the far-field scattering patterns, respectively.

IV. Results and Discussions

As previously mentioned, 2-bit programmable metasurfaces have been recently investigated to control EM waves in real time, such as breaking reciprocity [23], realizing dynamic beam manipulation [24], and machine-learning imager [25]. Here, we utilize the 2-bit programmable metasurface presented in Ref. [23] to validate the method and designs in Sections II and III. We firstly display the design of the PIN diode-based 2-bit programmable element, as illustrated in Fig. 10(a), which consists of an irregular hexagonal metal patch and two metal strips printed on the grounded F4B substrate ($\varepsilon_r = 2.65$ and $\tan\delta = 0.001$) with the thickness of 1.5mm. Two PIN diodes (MADP-000907-14020x from MACOM) are employed to connect the hexagonal patch with two strips, which serve as biasing lines for each diode. The hexagonal patch and the ground are connected through a metal via hole. The detailed parameters of the programmable elements are optimized to attain a 90° phase difference when two diodes switch among "OFF-OFF (00)", "OFF-ON (01)", "ON-OFF (10)", and "ON-ON (11)" states. Full-wave simulations are carried out by using the commercial software, CST Microwave Studio. In the simulations of the element, periodic boundary conditions are applied along both *x* and *y* directions, and two Floquet ports are used along the $\pm z$ directions. A normally incident plane wave illumination (with *x*-polarized electric field) is assumed to calculate the reflection coefficients of the element under different coding states. Fig. 11 shows the simulated reflection phases and amplitudes in the frequency range of 9.2-10.2 GHz, pertaining to the four coding states "00", "01", "10", and "11", respectively. We observe that the phase difference between

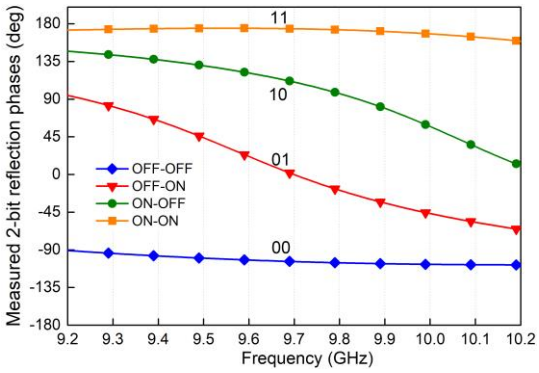

Fig. 13. Measured reflection phases of the 2-bit coding metasurface for four possible combinations of the diode states.

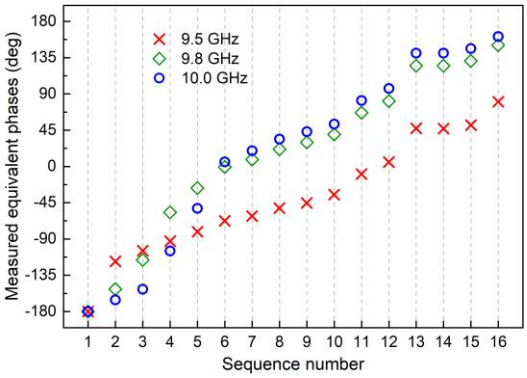

Fig. 14. The measured equivalent phases at different frequencies by using the sixteen sets of time-coding sequences in Fig. 3.

adjacent coding states is about 90° around 9.5 GHz, and the corresponding amplitudes are above 0.79.

Based on the design of elements, a prototype of the programmable metasurface in Ref. [23] was fabricated by low-cost printed circuit board (PCB) technology, as displayed in Fig. 10(b). This prototype is composed of two separate samples, each of which has eight columns with eight connected elements. Here, a single sample with 8×8 elements is firstly used to measure the reflection phases by a free space method under the normal incidence, a plane-wave lens antenna connected to a vector network analyzer (Keysight N5230C) is used to transmit and receive the signal, as shown in Fig. 12(a). Fig. 13 shows the measured reflection phases of the 2-bit coding states, in which the phase difference between adjacent coding states is not exactly 90° due to the unavoidable design imperfections and fabrication tolerances. When the FPGA controller provides the sixteen sets of time-coding sequences in Fig. 3(a), the equivalent reflection phases are measured at three different central frequencies, as shown in Fig. 14. In the view of the imperfect 2-bit phases in Fig. 13, there are some deviations in the equivalent 4-bit phases between the measured and theoretical results. Nevertheless, the equivalent 4-bit phases can still cover the range of -180° to 180° at the central frequency of 10 GHz.

Finally, we measure the scattering patterns of the original 2-bit programmable metasurface and the equivalent 4-bit phases of time-domain digital coding metasurface. The far-field measurements are carried out in a microwave anechoic chamber to obtain the scattering patterns of metasurface, as

This article has been accepted for publication in a future issue of this journal, but has not been fully edited. Content may change prior to final publication. Citation information: DOI 10.1109/TAP.2019.2955219, IEEE Transactions on Antennas and Propagation

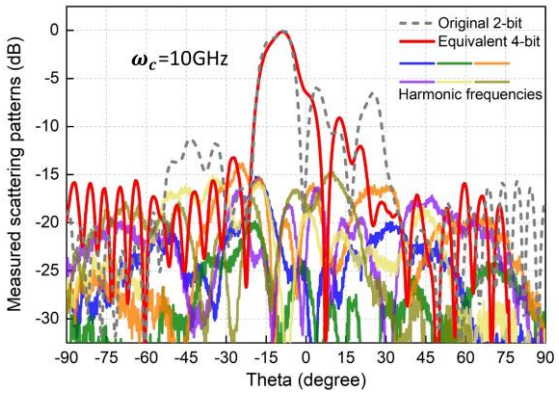

Fig. 15. Comparison of measured scattering patterns pertaining to the original 2-bit phases and the equivalent 4-bit phases in Fig. 3 for realizing beam steering at the central frequency.

shown in Fig. 12(b). A linearly polarized horn antenna provides the plane wave excitation and is connected to a signal generator (Keysight E8267D), while another linearly polarized horn antenna connected to a spectrum analyzer (Keysight E4447A) is used to receive the scattered harmonic signals. Besides, an FPGA hardware control board is exploited to provide dynamic biasing voltages for the 2-bit programmable metasurface. It can be seen that the time-domain coding metasurface with the equivalent 4-bit phases has better performance of beam steering at 10 GHz, in which the side lobes are much lower than that in the original 2-bit case, as shown in Fig. 15. Besides, the scattering powers at the harmonic frequencies are well suppressed to ensure the efficiency at the central frequency. The measured results agree well with the theoretical analyses, validating the effectiveness of the proposed time-domain coding approach.

V. Conclusion

We have proposed a time-varying approach based on 2-bit time-domain coding metasurface to achieve multi-bit and even quasi-continuous phase modulations at the central frequency or harmonic frequencies. By introducing the method of vector synthesis, we have demonstrated that the equivalent phases can be synthesized into arbitrary values with 360 °phase coverage, as long as the 2-bit time-coding sequences are suitably designed. Moreover, sixteen sets of time-coding sequences were applied to generate the equivalent 4-bit phases in the beam steering application, showing the advantage of reducing the quantization lobes. Finally, an FPGA-controlled prototype presented in Ref. [23] was utilized to experimentally validate the effectiveness of the proposed approach. Overall, our proposed time-varying coding strategy provides a simple way of designing arbitrary multi-bit programmable meta-devices, without the requirement of complicated structural design and control system, which may find significant applications to high-performance antennas, high-resolution imaging, as well as high-capacity wireless communications and radar systems. This approach can be extended to the terahertz, optical and acoustic regimes by exploring different implementations, and can be further generalized to achieve multi-bit transmission phases.

References

[1] S. Sun, Q. He, J. Hao, S. Xiao, and L. Zhou, "Electromagnetic metasurfaces: physics and applications," *Adv. Opt. Photonics*, vol. 11, no. 2, 2019.

[2] C. L. Holloway, E. F. Kuester, J. A. Gordon, J. O'Hara, J. Booth, and D. R. Smith, "An Overview of the Theory and Applications of Metasurfaces: The Two-Dimensional Equivalents of Metamaterials," *IEEE Antennas Propag. Mag.*, vol. 54, no. 2, pp. 10-35, Apr 2012.

[3] S. Sun, Q. He, S. Xiao, Q. Xu, X. Li, and L. Zhou, "Gradient-index meta-surfaces as a bridge linking propagating waves and surface waves," *Nat. Mater.*, vol. 11, no. 5, pp. 426-31, Apr 01 2012.

[4] N. K. Grady *et al.*, "Terahertz metamaterials for linear polarization conversion and anomalous refraction," *Science*, vol. 340, no. 6138, pp. 1304-7, Jun 14 2013.

[5] X. Zhang *et al.*, "Broadband terahertz wave deflection based on C-shape complex metamaterials with phase discontinuities," *Adv. Mater.*, vol. 25, no. 33, pp. 4567-72, Sep 06 2013.

[6] N. F. Yu *et al.*, "Light Propagation with Phase Discontinuities: Generalized Laws of Reflection and Refraction,", *Science*, vol. 334, no. 6054, pp. 333-337, Oct 21 2011.

[7] L. Huang *et al.*, "Dispersionless phase discontinuities for controlling light propagation," *Nano Lett.*, vol. 12, no. 11, pp. 5750-5755, Nov 14 2012.

[8] B. Assouar, B. Liang, Y. Wu, Y. Li, J.-C. Cheng, and Y. Jing, "Acoustic metasurfaces," *Nat. Rev. Mater.*, vol. 3, no. 12, pp. 460-472, 2018.

[9] T. J. Cui, M. Q. Qi, X. Wan, J. Zhao, and Q. Cheng, "Coding metamaterials, digital metamaterials and programmable metamaterials," *Light: Sci. Appl.*, vol. 3, no. 10, p. e218, Oct. 2014.

[10] T. J. Cui, S. Liu, and L. Zhang, "Information metamaterials and metasurfaces," *J. Mater. Chem. C*, vol. 5, no. 15, pp. 3644-3668, 2017.

[11] T. J. Cui, "Microwave metamaterials—from passive to digital and programmable controls of electromagnetic waves," *J. Opt.*, vol. 19, no. 8, p. 084004, 2017.

[12] T. J. Cui, "Microwave metamaterials," *Natl. Sci. Rev.*, vol. 5, no. 2, pp. 134-136, 2018.

[13] S. Liu *et al.*, "Convolution Operations on Coding Metasurface to Reach Flexible and Continuous Controls of Terahertz Beams," *Adv. Sci.*, vol. 3, no. 10, p. 1600156, Oct 2016.

[14] L. Zhang *et al.*, "Realization of Low Scattering for a High-Gain Fabry-Perot Antenna Using Coding Metasurface," *IEEE Trans. Antennas Propag.*, vol. 65, no. 7, pp. 3374-3383, Jul 2017.

[15] M. Moccia *et al.*, "Suboptimal Coding Metasurfaces for Terahertz Diffuse Scattering," *Sci. Rep.*, vol. 8, no. 1, p. 11908, Aug 9 2018.

[16] L. Zhang, S. Liu, L. Li, and T. J. Cui, "Spin-Controlled Multiple Pencil Beams and Vortex Beams with Different Polarizations Generated by Pancharatnam-Berry Coding Metasurfaces," *ACS Appl. Mater. Interfaces*, vol. 9, no. 41, pp. 36447-36455, Oct 18 2017.

[17] S. Liu *et al.*, "Anomalous Refraction and Nondiffractive Bessel-Beam Generation of Terahertz Waves through Transmission-Type Coding Metasurfaces," *ACS Photonics*, vol. 3, no. 10, pp. 1968-1977, 2016.

[18] L. Zhang *et al.*, "Transmission-Reflection-Integrated Multifunctional Coding Metasurface for Full-Space Controls of Electromagnetic Waves," *Adv. Funct. Mater.*, vol. 28, no. 33, p. 1802205, 2018.

[19] B. Xie, K. Tang, H. Cheng, Z. Liu, S. Chen, and J. Tian, "Coding Acoustic Metasurfaces," *Adv. Mater.*, vol. 29, no. 6, Feb 2017.

[20] X. Wan, M. Q. Qi, T. Y. Chen, and T. J. Cui, "Field-programmable beam reconfiguring based on digitally-controlled coding metasurface," *Sci. Rep.*, vol. 6, p. 20663, Feb 10 2016.

[21] H. Yang *et al.*, "A programmable metasurface with dynamic polarization, scattering and focusing control," *Sci. Rep.*, vol. 6, p. 35692, Oct 24 2016.

[22] L. Zhang *et al.*, "Space-time-coding digital metasurfaces," *Nat. Commun.*, vol. 9, no. 1, p. 4334, Oct 18 2018.

[23] L. Zhang et al., "Breaking Reciprocity with Space-Time-Coding Digital Metasurfaces," *Adv. Mater.*, vol. 31, no. 41, p. 1904069, 2019.

[24] C. Huang, B. Sun, W. Pan, J. Cui, X. Wu, and X. Luo, "Dynamical beam manipulation based on 2-bit digitally-controlled coding metasurface," *Sci. Rep.*, vol. 7, p. 42302, Feb 08 2017.

[25] L. Li *et al.*, "Machine-learning reprogrammable metasurface imager," *Nat. Commun.*, vol. 10, no. 1, 2019.

[26] B. Wu, A. Sutinjo, M. E. Potter, and M. Okoniewski, "On the selection of the number of bits to control a dynamic digital MEMS reflectarray," *IEEE Antennas Wireless Propag. Lett.*, vol. 7, pp. 183–186, 2008.

[27] C. R. Dietlein, A. S. Hedden, and D. A. Wikner, "Digital reflectarray considerations for terrestrial millimeter wave imaging," *IEEE Antennas*

Wireless Propag. Lett., vol. 11, pp. 272–275, 2012.
[28] Q. Wu and R. Zhang, "Beamforming optimization for intelligent reflecting surface with discrete phase shifts," in *Proc. IEEE ICASSP*, May 2019, pp. 7830–7833.
[29] K. Chen *et al.,* "A Reconfigurable Active Huygens' Metalens," *Adv. Mater.,* vol. 29, no. 17, May 2017.
[30] Z. Wu, Y. Ra'di, and A. Grbic, "Tunable Metasurfaces: A Polarization Rotator Design," *Phys. Rev. X*, vol. 9, no. 1, 2019.
[31] W. Tang et al., "Programmable metasurface-based RF chain-free 8PSK wireless transmitter," *Electron. Lett.*, vol. 55, no. 7, pp. 417-420, 2019.
[32] J. Zhao *et al.,* "Programmable time-domain digital-coding metasurface for non-linear harmonic manipulation and new wireless communication systems," *Natl. Sci. Rev.,* vol. 6, no. 2, pp. 231-238, 2019.
[33] J. Y. Dai, J. Zhao, Q. Cheng, and T. J. Cui, "Independent control of harmonic amplitudes and phases via a time-domain digital coding metasurface," *Light: Sci. Appl.,* vol. 7, no. 1, p. 90, 2018.
[34] L. Cong, P. Pitchappa, C. Lee, and R. Singh, "Active Phase Transition via Loss Engineering in a Terahertz MEMS Metamaterial," *Adv. Mater.,* vol. 29, no. 26, Jul 2017.
[35] Z. Miao *et al.,* "Widely Tunable Terahertz Phase Modulation with Gate-Controlled Graphene Metasurfaces," *Phys. Rev. X,* vol. 5, no. 4, 2015.
[36] B. Y. Wei *et al.,* "Generating switchable and reconfigurable optical vortices via photopatterning of liquid crystals," *Adv. Mater.,* vol. 26, no. 10, pp. 1590-5, Mar 12 2014.
[37] L. Wang *et al.,* "A Review of THz Modulators with Dynamic Tunable Metasurfaces," *Nanomaterials,* vol. 9, no. 7, 2019..
[38] Y.-W. Huang *et al.,* "Structured Semiconductor Interfaces: Active Functionality on Light Manipulation," *Proc. IEEE,* pp. 1-23, 2019.
[39] A. Shaltout, A. Kildishev, and V. Shalaev, "Time-varying metasurfaces and Lorentz non-reciprocity," *Opt. Mater Express*, vol. 5, no. 11, p. 2459, 2015.
[40] D. L. Sounas and A. Alù, "Non-reciprocal photonics based on time modulation," *Nat. Photonics,* vol. 11, no. 12, pp. 774-783, 2017.
[41] M. M. Salary, S. Jafar-Zanjani, and H. Mosallaei, "Electrically tunable harmonics in time-modulated metasurfaces for wavefront engineering," *New J. Phys.*, vol. 20, no. 12, 2018.
[42] D. Ramaccia, D. L. Sounas, A. Alu, A. Toscano, and F. Bilotti, "Metasurface-based Doppler cloaks: Time-varying metasurface profile to achieve perfect frequency mixing," in *2018 12th International Congress on Artificial Materials for Novel Wave Phenomena (Metamaterials)*, 2018, pp. 331–333.
[43] Z. Wu and A. Grbic, "A Transparent, Time-Modulated Metasurface," in *2018 12th International Congress on Artificial Materials for Novel Wave Phenomena (Metamaterials)*, 2018, pp. 439–441.
[44] Z. Wu, and A. Grbic,"Serrodyne frequency translation using time-modulated metasurfaces." *arXiv prepr. arXiv*:1905.06792 (2019).
[45] J. W. Zang, D. Correas-Serrano, J. T. S. Do, X. Liu, A. Alvarez-Melcon, and J. S. Gomez-Diaz, "Nonreciprocal Wavefront Engineering with Time-Modulated Gradient Metasurfaces," *Phys. Rev. Appl.*, vol. 11, no. 5, 2019.
[46] Y. Hadad, D. L. Sounas, and A. Alu, "Space-time gradient metasurfaces," *Phys. Rev. B,* vol. 92, no. 10, 2015.
[47] Y. Hadad, J. C. Soric, and A. Alu, "Breaking temporal symmetries for emission and absorption," *Proc. Natl. Acad. Sci.*, vol. 113, no. 13, pp. 3471–3475, Mar. 2016
[48] A. M. Shaltout, V. M. Shalaev, and M. L. Brongersma, "Spatiotemporal light control with active metasurfaces," *Science*, vol. 364, no. 6441, May 17 2019.
[49] S. Taravati and A. A. Kishk, "Space-Time Modulation: Principles and Applications." *arXiv prepr. arXiv*:1903.01272, 2019.
[50] S. Taravati, "Giant Linear Nonreciprocity, Zero Reflection, and Zero Band Gap in Equilibrated Space-Time-Varying Media," *Phys. Rev. Appl.*, vol. 9, no. 6, 2018.
[51] D. Ramaccia, D. L. Sounas, A. Alu, A. Toscano, and F. Bilotti, "Doppler cloak restores invisibility to objects in relativistic motion," *Phys. Rev. B*, vol. 95, no. 7, Feb 6 2017.
[52] S. Taravati and A. A. Kishk, "Advanced Wave Engineering via Obliquely Illuminated Space-Time-Modulated Slab," IEEE Transactions on Antennas and Propagation, vol. 67, no. 1, pp. 270-281, 2019.
[53] S. Taravati, N. Chamanara, and C. Caloz, "Nonreciprocal electromagnetic scattering from a periodically space-time modulated slab and application to a quasisonic isolator," *Phys. Rev. B*, vol. 96, no. 16, 2017.
[54] D. Ramaccia, D. L. Sounas, A. Alù, F. Bilotti, and A. Toscano, "Nonreciprocal Horn Antennas Using Angular Momentum-Biased Metamaterial Inclusions," *IEEE Trans. Antennas Propag.*, vol. 63, no. 12, 2015.
[55] D. Ramaccia, D. L. D. L. Sounas, A. Alu, F. Bilotti, and A. Toscano, "Nonreciprocity in antenna radiation induced by space-time varying metamaterial cloaks," *IEEE Antennas Wirel. Propag. Lett.*, vol. 17, no. 11, pp. 1968–1972, Nov. 2018.
[56] D. Correas-Serrano, J. S. Gomez-Diaz, D. L. Sounas, Y. Hadad, A. Alvarez-Melcon, and A. Alu, "Nonreciprocal Graphene Devices and Antennas Based on Spatiotemporal Modulation," *IEEE Antennas Wirel. Propag. Lett.*, vol. 15, pp. 1529-1532, 2016
[57] S. Taravati, and C. Caloz, "Mixer-Duplexer-Antenna Leaky-Wave System Based on Periodic Space-Time Modulation," *IEEE Trans. Antennas Propag.*, vol. 65, no. 2, pp. 442-452, 2017.
[58] S. Taravati and G. V. Eleftheriades, "Generalized Space-Time-Periodic Diffraction Gratings: Theory and Applications," *Phys. Rev. Appl.*, vol. 12, no. 2, 2019.
[59] R. J. Mailloux, *Phased Array Antenna Handbook*, 2nd ed. Boston, MA: Artech House, 2005.

Lei Zhang was born in Anhui, China, in 1992. He received the B.E. degree in electromagnetic wave propagation and antenna from Xidian University, Xi'an, China, in 2015. He is currently pursuing the Ph.D. degree in electromagnetic field and microwave technology at the State Key Laboratory of Millimeter Waves, Southeast University, Nanjing, China.

He has authored or co-authored over 25 peer-reviewed journal papers. His current research interests include metamaterials, antenna design and space-time-modulated metadevices. Mr. Zhang was a recipient of Best Student Paper Award at the 6th Asia-Pacific Conference on Antennas and Propagation (APCAP) in 2017.

Zheng Xing Wang received the B.Sc. degree in electromagnetics and microwave technology from Xidian University, Xi'an, China, in 2017. He is currently pursuing the M.S. degree with Southeast University, Nanjing, China. His current interests include spoof surface plasmons, metasurface, and transmit-array and reflect-array antenna.

Rui Wen Shao was born in Jiangsu, China, in 1997. He received the B.E. degree in information engineering from Southeast University, Nanjing, China, in 2019. He is currently pursuing the M.S. degree in electromagnetic field and microwave technology with the State Key Laboratory of Millimeter Waves, Southeast University, Nanjing, China. His current research interests include metasurfaces and antenna array.

Jia Lin Shen was born in Hunan, China, in 1997. She received the B.E. degree in electronic information science and technology from Xidian University, Xi'an, China, in 2018. She is currently pursuing the M.S. degree in electromagnetic field and microwave technology with the State Key Laboratory of Millimeter Waves, Southeast University, Nanjing, China. Her current research interests include metasurfaces and antenna array.

Xiao Qing Chen received the B.S. degree in electronic science and technology and M.S. degree in electromagnetic field and microwave technology from Southeast University, Nanjing, China, in 2015 and 2018, respectively.

She is now an RF engineer with Huawei Technologies. Her current research interests include microwave/millimeter-wave passive components, antennas and metamaterials.

This article has been accepted for publication in a future issue of this journal, but has not been fully edited. Content may change prior to final publication. Citation information: DOI 10.1109/TAP.2019.2955219, IEEE Transactions on Antennas and Propagation

Xiang Wan was born in Hubei, China, in 1986. He received the B.E. degree in electrical and information engineering and the M.E. degree in electromagnetic field and microwave technology from Wuhan University, Wuhan, China, in 2007 and 2010, respectively, and the Ph.D. degree in electromagnetic field and microwave technology from Southeast University, Nanjing, China, in 2014.

Since 2014, he has been a Faculty Member with the School of Information Science and Engineering, Southeast University. His current research interests include programmable metasurfaces, low-profile antennas and antenna arrays.

Qiang Cheng (M'15) received the B.S. and M.S. degrees from the Nanjing University of Aeronautics and Astronautics, Nanjing, Jiangsu, China, in 2001 and 2004, respectively, and the Ph.D. degree from Southeast University, Nanjing, in 2008.

In 2008, he joined the State Key Laboratory of Millimeter Waves, Southeast University, where he was involved in the development of metamaterials and metadevices. He is currently a Full Professor with the Radio Department, Southeast University. He leads a group of Ph.D. students and master students in the area of metamaterials, tunable microwaves circuits, microwave imaging, and terahertz systems. He has authored or co-authored more than one hundred publications, with citation over 2000 times.

Dr. Cheng was a recipient of the 2010 Best Paper Award from the New Journal of Physics, the Chinas Top Ten Scientific Advances of 2010, and the Second Class National Natural Science Award in 2014. He served as the Vice Chair for the 2008 and 2010 International Workshop on Metamaterials, Nanjing, China.

Tie Jun Cui (M'98-SM'00-F'15) received the B.Sc., M.Sc., and Ph.D. degrees in electrical engineering from Xidian University, Xi'an, China, in 1987, 1990, and 1993, respectively. In March 1993, he joined the Department of Electromagnetic Engineering, Xidian University, and was promoted to an Associate Professor in November 1993. From 1995 to 1997 he was a Research Fellow with the Institut fur Hochstfrequenztechnik und Elektronik (IHE) at the University of Karlsruhe, Germany. In July 1997, he joined the Center for Computational Electromagnetics, Department of Electrical and Computer Engineering, University of Illinois at Urbana-Champaign, first as a Postdoctoral Research Associate and then a Research Scientist. In September 2001, he was a Cheung-Kong Professor with the Department of Radio Engineering, Southeast University, Nanjing, China. From January 2018, he became Chief Professor of Southeast University.

Dr. Cui is the first author of books Metamaterials – Theory, Design, and Applications (Springer, Nov. 2009) and Metamaterials: Beyond Crystals, Noncrystals, and Quasicrystals (CRC Press, Mar. 2016). He has published over 500 peer-review journal papers, which have been cited by more than 25000 times (H-Factor 79; from Google Scholar), and licensed over 60 patents. Dr. Cui was awarded a Research Fellowship from the Alexander von Humboldt Foundation, Bonn, Germany, in 1995, received a Young Scientist Award from the International Union of Radio Science in 1999, was awarded a Cheung Kong Professor under the Cheung Kong Scholar Program by the Ministry of Education, China, in 2001, and received the National Science Foundation of China for Distinguished Young Scholars in 2002. Dr. Cui received the Natural Science Award (first class) from the Ministry of Education, China, in 2011, and the National Natural Science Awards of China (second class), in 2014 and 2018, respectively. His researches have been selected as one of the most exciting peer-reviewed optics research "Optics in 2016" by Optics and Photonics News Magazine (OSA), 10 Breakthroughs of China Science in 2010, "Best of 2010" in New Journal of Physics, and Research Highlights in a series of journals. His work has been widely reported by Nature News, MIT Technology Review, Scientific American, Discover, New Scientists, etc.

Dr. Cui is an IEEE Fellow, and was an Associate Editor in IEEE Transactions on Geoscience and Remote Sensing, Guest Editor in Science China - Information Sciences, Guest Editor in Science Bulletin, and Guest Editor in Research. He served as General Co-Chair of the International Workshops on Metamaterials (META'2008, META'2012), TPC Co-Chair of Asian Pacific Microwave Conference (APMC'2005), TPC Co-Chair of Progress in Electromagnetic Research Symposium (PIERS'2004), and TPC Member of the International Congress on Advanced Electromagnetic Materials in Microwaves and Optics (Metamaterials'2014, 2016, 2018, 2019). He presented more than 30 Keynote and Plenary Talks in Academic Conferences, Symposiums, or Workshops.